View metadata, citation and similar papers at core.ac.uk
brought to you by CORE
provided by Digital Commons @ West Chester University

West Chester University
Digital Commons @ West Chester University

Chemistry | College of the Sciences & Mathematics

1-9-2017

Regenerative Electroless Etching of Silicon

Kurt W. Kolasinski
West Chester University of Pennsylvania, kkolasinski@wcupa.edu

Nathan J. Gimbar
West Chester University of Pennsylvania

Haibo Yu
University of Connecticut - Storrs

Mark Aindow
University of Connecticut - Storrs

Ermei Mäkilä
University of Turku

See next page for additional authors

Follow this and additional works at: https://digitalcommons.wcupa.edu/chem_facpub

Part of the Materials Chemistry Commons

Recommended Citation

Kolasinski, K. W., Gimbar, N. J., Yu, H., Aindow, M., Mäkilä, E., & Salonen, J. (2017). Regenerative Electroless Etching of Silicon. *Angewandte Chemie International Edition, 129*(2), 639-642. http://dx.doi.org/10.1002/ange.201610162

This Article is brought to you for free and open access by the College of the Sciences & Mathematics at Digital Commons @ West Chester University. It has been accepted for inclusion in Chemistry by an authorized administrator of Digital Commons @ West Chester University. For more information, please contact wcressler@wcupa.edu.

Authors
Kurt W. Kolasinski, Nathan J. Gimbar, Haibo Yu, Mark Aindow, Ermei Mäkilä, and Jarno Salonen

This article is available at Digital Commons @ West Chester University: https://digitalcommons.wcupa.edu/chem_facpub/20

Regenerative Electroless Etching of Silicon

Kurt W. Kolasinski,*[a] Nathan J. Gimbar,[a] Haibo Yu,[b] Mark Aindow,[b] Ermei Mäkilä,[c] and Jarno Salonen[c]

Abstract: Regenerative electroless etching (ReEtching), described here for the first time, is a method of producing nanostructured semiconductors in which an oxidant (Ox_1) is used as a catalytic agent to facilitate reaction between a semiconductor and a second oxidant (Ox_2) that would be unreactive in the primary reaction. Ox_2 is used to regenerate Ox_1, which is capable of initiating etching by injecting holes into the semiconductor valence band. Thereby the extent of reaction is controlled by the amount of Ox_2 added and the rate of reaction is controlled by the injection rate of Ox_2. This general strategy is demonstrated specifically for the production of highly luminescent, nanocrystalline porous Si from the reaction of V_2O_5 in HF(aq) as Ox_1 and H_2O_2(aq) as Ox_2 with Si powder and wafers.

Numerous applications of nanostructured silicon,[1] e.g. consumer products, nanomedicine[2] and rechargeable batteries,[3] would benefit from economical production of porous powder on the kilogram to ton scale. Electroless etching of metallurgical grade Si (\$1 kg^{-1} vs. \$10,000 kg^{-1} for semiconductor grade Si) is recognized as a process with tremendous industrial potential but only if issues related to reproducibility, controllability, purity, cost and scaling can be addressed.[4] HNO_3-based-processes suffer with an inability to produce specific surface area >150 m^3 g^{-1}, incomplete etching of particles and a yield of 5%.[4b, 5] Replacement of HNO_3 by Fe^{3+},[6] led to production of powders with much greater specific surface area (up to 408 m^2 g^{-1}) and improved yield (h £ 0.24, defined as the ratio of final mass to initial mass);[4c, 7] though issues with process control (particularly thermal budget, drying, salt precipitation) and cost remain.

We introduce a new concept in electroless etching, potentially applicable to any semiconductor, which we apply to the formation of nanostructured Si. We demonstrate production of high specific surface area (>400 m^2 g^{-1}) photoluminescent porous Si (por-Si). The strategy uses a catalytic amount of V_2O_5 dissolved in HF(aq), which produces VO_2^+. This acts as the primary oxidant Ox_1 that injects holes into the Si valence band, a necessary condition for nanostructuring.[8] VO_2^+ is an optimal oxidant for the initiation of Si electroless etching.[9] For example, using the data of Gondek et al. [10] to that of Ref. [11], we show in the supplemental information that the rate of etching induced by VO_2^+ exceeds the etch rate induced by H_2O_2 by more than a factor of 4000. Unexpectedly, the oxidant plays two roles: (i) it initiates etching by hole injection, and (ii) it consumes a conduction band electron injected by a fluoride reaction intermediate.[12] This doubles the oxidant-associated cost because two moles are consumed per mole Si etched instead of the 1:1 ratio previously assumed. Importantly, the technique we introduce allows us to use H_2O_2 (\$0.5 kg^{-1}) – an oxidant that is known *not* to produce porous Si in the absence of a metal particle catalyst [10, 13] – in place of the vast majority of V_2O_5 (\$50 kg^{-1}), which simultaneously enhances economic viability and process control (reducing heating and eliminating precipitation).

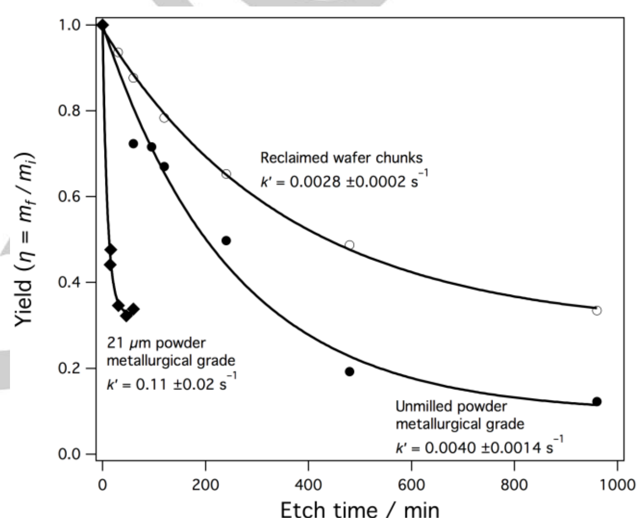

Figure 1. Exponential decay of yield versus time indicates pseudo-first order kinetics for etching in V_2O_5+HF solution regardless of whether the Si sample is composed of crushed semiconductor-grade wafers, unmilled metallurgical grade granules or finely milled metallurgical grade powder.

We began etching with V_2O_5 + HF solutions containing a stoichiometric 2:1 molar ratio of V:Si. Figure 1 demonstrates the well-behaved kinetics of Si etched electrolessly in V_2O_5 + HF aqueous solutions at 0 °C. Three different types of Si were etched to produce the data in Fig. 1: crushed wafer reclaim (irregular rectangular shards hundreds of μm across), unmilled metallurgical grade powder (irregular rectangular particles broadly distributed about 500 μm and above), and milled metallurgical grade Si with a roughly Gaussian size distribution centered about 21 μm. All three exhibit simple exponential decay of the yield. This is consistent with pseudo-first-order kinetics. Si wafer etching in V_2O_5 + HF is first order in [V_2O_5] with a flat etch front.[11] The flat etch front means that the surface area that is being etched, which corresponds to the surface area of the pore tips, is roughly constant after pore initiation. As shown in the Supplemental Information, this combination should follow pseudo-first-order kinetics. We conclude that stain etching of powders and wafers follow the same etch dynamics even with the presence of impurities and polycrystallinity. Nonetheless, powder etching is much faster than wafer etching. The true rate constant for etching of the 21–μm powder is k = 0.45±0.08 m^{-2} s^{-1} at 273 K. Using the measured[12] activation energy of 30 ± 5

[a] Prof. K.W. Kolasinski (Corresponding Author) and N.J. Gimbar
Department of Chemistry
West Chester University
West Chester, PA 19383-2115 USA
E-mail: kkolasinski@wcupa.edu
[b] H. Yu and Prof. M. Aindow
Department of Materials Science & Engineering
University of Connecticut
Storrs, CT 06269-3136 USA
[c] E. Mäkilä and Dr. J. Salonen
Department of Physics
University of Turku
FI-20014 Turku, Finland

Supporting information for this article is given via a link at the end of the document.

kJ mol^{-1} for single-crystal Si to adjust a value obtained at 298 K, the true rate constant for etching Si wafer is $k = 0.036 \pm 0.010$ m^{-2} s^{-1} at 273 K. The presence of defects in metallurgical grade Si powder increased the etch rate by roughly one order of magnitude compared to wafer Si.

After rinsing with 0.2 M HCl(aq) then pentane during filtration, the powders were dried under vacuum. Upon exposure to the atmosphere the powders exhibited brilliant photoluminescence (PL) in the green-yellow region of the spectrum. The peak wavelength when excited at 350 nm varied in the range of 540–590 nm. However, the PL intensity decreased over the course of several days and red shifted to the range 600–650 nm. It finally stabilized after approximately a week. The specific surface area was up to 225 m^2 g^{-1}, much better than for HNO_3 etches but less than the best values reported for Fe^{3+} etching.

Scanning electron microscopy (SEM) and transmission electron microscopy (TEM) revealed the cause of moderate specific surface area and PL fading. Only a thin (hundreds of nm) layer of porous Si surrounds a solid core. This layer was fragile, which made the PL unstable. The solid core reduced both the porosity and specific surface area. Nonoptimal etching occured because the etch rate was too great, which effectively burned off (electropolished) some of the porous Si layer. When the concentration of oxidant dropped to a sufficiently low value, the net rate of film formation was positive. However, at this point there is too little oxidant left to make a thick film.

The system poses a conundrum. The amount of Si etched is determined by the amount of oxidant but the etch rate depends on concentration. Low concentrations (required to avoid electropolishing) coupled with a large amount of oxidant (required to etch sufficient Si) translate into large etchant volumes and long processing times. An effective, scalable process requires fundamental rethinking of how to etch.

Under optimal conditions etching occurs only at the pore tips, particle size is constant, and the volume etched equals the pore volume. The ratio of pore volume to particle volume defines the porosity ε. The fraction of remaining Si is defined by the mass loss ratio (*MLR*), which is one minus the yield, $MLR = 1 - \eta$. We define the optimal etch parameter *OEP* as the ratio of porosity ε to *MLR*. An optimal etch corresponds to *OEP* = 1, which means that all etching leads to pore formation rather than particle dissolution. With *OEP* ≈ 0.4, the powders produced with etches reported in Fig. 1, i.e. stoichiometric V_2O_5 added at the beginning of the etch, were significantly better than HNO_3 etching with *OEP* ≈ 0.3 but still not as good as the best reported by Loni et al.[4c, 7] with Fe^{3+}, which corresponds to *OEP* =0.66.

The V(V) species that initiates etching is converted quantitatively to V(IV).[12] This is accompanied by a color change from pale yellow to blue. The associated standard reduction potential is $E^\circ\left(VO_2^+/VO^{2+}\right) = 0.991$ V. We observed that when we added H_2O_2, $E^\circ\left(H_2O_2/H_2O\right) = 1.776$ V, to a blue V(IV) containing solution, the solution immediately turned red-brown. A similar color was obtained when H_2O_2 was added to a VO_2^+ solution. The ability of the red-brown solution to etch Si was confirmed by immediate bubble production upon addition of Si. We conclude that the red-brown solution corresponds to an oxovanadium(V) ion in solution, which is not VO_2^+ but is nonetheless capable of injecting holes into the Si valence band.

A totally new etch strategy is now at hand. This allows us to control the rate and the amount of etching independent of the amount of V_2O_5. We call this *regenerative electroless etching* (ReEtching). A catalytic amount of V_2O_5 is added to HF. Typically we use 0.05–0.5 g compared to the 6.5 g required by stoichiometry to etch 1 g of Si. After initiation of etching by mixing of V_2O_5 + HF with Si dispersed in HF + H_2O, we add H_2O_2 via a syringe pump. H_2O_2 regenerates the oxidant that initiates electroless etching. The injection rate controls the rate of etching. The amount of Si etched is controlled by the amount of H_2O_2. This allows us to replace 95% or more of the 100x more expensive V_2O_5. Slow continuous addition of H_2O_2 reduces the thermal load on the system and produces a steady state etch rate that allows for film formation with minimal electropolishing.

Using this method we have etched 4 µm powder (as opposed to the 2 µm powder used by Loni et al.) to 392 m^2 g^{-1} specific surface area, 3.2 nm mean pore diameter, 0.312 cm^3 pore volume, $\varepsilon = 0.421$, *MLR* = 0.822, *OEP* = 0.512 in a 160 min etch. Addition of acetic acid is found to increase *OEP*. For example, we achieved 403 m^2 g^{-1} specific surface area, 3.8 nm mean pore diameter, 0.388 cm^3 pore volume, $\varepsilon = 0.475$, *MLR* = 0.658, *OEP* = 0.721 in a 90 min etch. Scaling of the process to large batches is made much easier because the thermal load is greatly reduced. Furthermore, oxovanadium ions exhibit higher solubility than the ferric/ferrous system and H_2O_2 does not add precipitating ions. No precipitates are formed.

Considerable room for process optimization remains as we have only begun to explore the effects of initial concentration of V_2O_5, pump rate (which also determines etch time), ratio of H_2O_2 to Si, temperature, amount of H_2O and CH_3COOH added to HF, and, importantly, filtering, rinsing and drying conditions. Specific surface area increased with longer etch times but was reduced if a superstoichiometric amount of H_2O_2 was added. Addition of acetic acid (volume ratios of acetic acid: water: HF of 1:3:4) significantly increased the specific surface area and *OEP*. Acetic acid is a surfactant that decreased the etch rate while enhancing release of H_2 bubbles and replacement of etchant during rinsing. Porous particles are denser in the presence of acetic acid as evidenced by reduced foaming and floating because the pores contain less gas. Less gas and more etchant in the pores enhances etching as the pore tip relative to etching of the external surface. Therefore the *OEP* value was improved.

ReEtching 4 µm powder led to a mixture of single-crystal completely porosified, Fig. 2a, and porous shell/solid-core particles, Fig. 2b. Critically, electron diffraction revealed no amorphitization or pore collapse resulting from pentane drying. The porous shell in Fig. 2b exhibts banding. The mixture of completely etched and partially etched particles accompanied by banding were both related to inhomogeneous mixing caused by foaming. Some particles remained submerged until they etched completely. Other particles moved between etchant and foam with reduced effective etch time and less homogeneous etching. Increased stability of the porous layer was corroborated by PL. ReEtched por-Si was still subject to redshifting and intensity

decrease upon prolonged air exposure, however, the redshift was usually to 600–615 nm and significantly more intensity was retained (Supplemental Information). Air exposure also led to significant PL intensity in a blue band at ~485 nm.

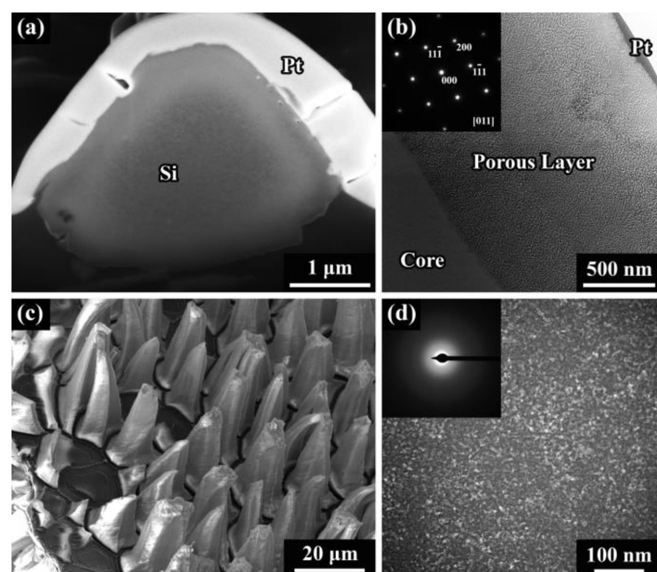

Figure 2. (a) Secondary electron (SE) SEM image of FIB-sectioned ~4 μm powder etched in V_2O_5 + H_2O_2 + HF reveals that is porosified to the core. (b) Bright-field (BF) TEM image obtained from a partially etched particle reveals banding in the porous layer outside of a solid core, and a selected area diffraction pattern (SADP) from the porous layer (inset) indicates it is single-crystalline. (c) SE SEM image reveals ~20 μm tall pillars etched into a ~1 mm powder particle during ReEtching for 6h. (d) BF TEM image obtained from a single pillar reveals it to be porous, and the SADP (inset) reveals it to be totally amorphous. The region below the pillars was porous to a depth extending over 2 μm (supplemental material).

The versatility of ReEtching opens up previously unattainable processing capabilities. Foaming is extreme for 4 μm and smaller particles but decreases for increasing particle size. By achieving the appropriate steady-state etch rate with an optimized combination of V_2O_5 and H_2O_2, we can etch larger particles effectively. Results in Figs. 2c and 2d demonstrate that porosification to a depth >20 μm on one side of a particle has been achieved. This is important because between 21 μm and 100 μm, foaming disappears completely even without addition of acetic acid allowing for homogeneous complete etching.

ReEtching can be applied to other starting materials including wafers and to por-Si powder produced by magnesiothermal reduction,[14] or pulverization of anodized wafers.[15] Mesoporous powder produced by anodization, which was not initially photoluminescent, was ReEtched. This allowed us to introduce much smaller quantum-confined structures within the ~14 nm mesopores. The result was stunningly bright and persistent photoluminescent material as shown in Figure S3.

Regenerative electroless etching (ReEtching) is a process in which one oxidant is used to regenerate a more reactive but costly oxidant. We have demonstrated that ReEtching provides previously unattainable processing control over electroless etching and the realization of effective, low-cost bulk synthesis of nanocrystalline porous Si powder.

Experimental Section

Porous Si samples have been made in West Chester and Turku with reagents from multiple sources, see Supplemental Information for details.

Acknowledgements

Funding: Academy of Finland (277190) and West Chester University FaStR program. Microscopy studies were performed using the facilities in the UConn/FEI Center for Advanced Microscopy and Materials Analysis (CAMMA). Vesta Sciences and Jim Falcone provided Si powders and wafer chunks.

Keywords: nanostructure • porous silicon • electroless etching • photoluminescence • electrochemistry

[1] a J. R. Henstock, L. T. Canham, S. I. Anderson, *Acta Biomater* **2015**, *11*, 17-26; b L. T. Canham, in *Handbook of Porous Silicon*, 2nd ed. (Ed.: L. T. Canham), Springer Verlag, Berlin, **2014**, pp. 733-740.
[2] H. A. Santos, E. Mäkilä, A. J. Airaksinen, L. M. Bimbo, J. Hirvonen, *Nanomedicine* **2014**, *9*, 535-554.
[3] H. Wu, Y. Cui, *Nano Today* **2012**, *7*, 414-429.
[4] a X. Li, J.-H. Lee, A. N. Sprafke, R. B. Wehrspohn, *Semicond. Sci. Technol.* **2016**, *31*, 014009; b E. G. Chadwick, N. V. V. Mogili, C. O'Dwyer, J. D. Moore, J. S. Fletcher, F. Laffir, G. Armstrong, D. A. Tanner, *Rsc Adv* **2013**, *3*, 19393-19402; c A. Loni, D. Barwick, L. Batchelor, J. Tunbridge, Y. Han, Z. Y. Li, L. T. Canham, *Electrochem. Solid State Lett.* **2011**, *14*, K25-K27.
[5] a E. G. Chadwick, S. Beloshapkin, D. A. Tanner, *J. Mater. Sci.* **2012**, *47*, 2396-2404; b S. Limaye, S. Subramanian, B. Goller, J. Diener, D. Kovalev, *Phys. Status Solidi A* **2007**, *204*, 1297-1301.
[6] a M. E. Dudley, K. W. Kolasinski, *Electrochem. Solid State Lett.* **2009**, *12*, D22-D26; b M. Nahidi, K. W. Kolasinski, *J. Electrochem. Soc.* **2006**, *153*, C19-C26.
[7] M. Wang, P. S. Hartman, A. Loni, L. T. Canham, J. L. Coffer, *Silicon* **2016**, *8*, 525-531.
[8] a K. W. Kolasinski, *Curr. Opin. Solid State Mater. Sci.* **2005**, *9*, 73-83; b K. W. Kolasinski, *Phys. Chem. Chem. Phys.* **2003**, *5*, 1270-1278.
[9] a K. W. Kolasinski, J. W. Gogola, W. B. Barclay, *J. Phys. Chem. C* **2012**, *116*, 21472–21481; b K. W. Kolasinski, J. W. Gogola, *ECS Trans.* **2011**, *33*, 23-28.
[10] C. Gondek, M. Lippold, I. Röver, K. Bohmhammel, E. Kroke, *J. Phys. Chem. C* **2014**, *118*, 2044-2051.
[11] K. W. Kolasinski, J. D. Hartline, B. T. Kelly, J. Yadlovskiy, *Mol. Phys.* **2010**, *108*, 1033-1043.
[12] K. W. Kolasinski, W. B. Barclay, *Angew. Chem., Int. Ed. Engl.* **2013**, *52*, 6731-6734.
[13] a H. Seidel, L. Csepregi, A. Heuberger, H. Baumgärtel, *J. Electrochem. Soc.* **1990**, *137*, 3612-3626; b U. Neuwald, A. Feltz, U. Memmert, R. J. Behm, *J. Appl. Phys.* **1995**, *78*, 4131-4136; c H. G. G. Philipsen, J. J. Kelly, *Electrochim. Acta* **2009**, *54*, 3526-3531; d Z. Huang, N. Geyer, P. Werner, J. de Boor, U. Gösele, *Adv. Mater.* **2011**, *23*, 285-308; e X. L. Li, *Curr. Opin. Solid State Mater. Sci.* **2012**, *16*, 71-81.
[14] L. Batchelor, A. Loni, L. T. Canham, M. Hasan, J. L. Coffer, *Silicon* **2012**, *4*, 259-266.
[15] C.-F. Wang, M. P. Sarparanta, E. M. Mäkilä, M. L. K. Hyvonen, P. M. Laakkonen, J. J. Salonen, J. T. Hirvonen, A. J. Airaksinen, H. A. Santos, *Biomaterials* **2015**, *48*, 108-118.

ACCEPTED MANUSCRIPT

Entry for the Table of Contents (Please choose one layout)

Layout 1:

COMMUNICATION

H_2O_2 regenerates V in a 5+ oxidation state, which initiates etching to produce porous Si powder containing fully etched particles.

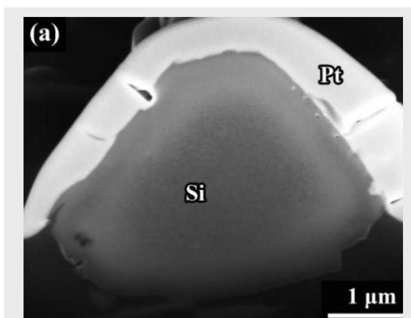

Kurt W. Kolasinski, Nathan J. Gimbar, Haibo Yu, Mark Aindow, Ermei Mäkilä, and Jarno Salonen*

Page No. – Page No.

Regenerative Electroless Etching of Silicon

WILEY-VCH